On new alkaline earth hexafluorogermanates as host structures for UV phosphors

Martin J. Schäfer, Florian Fleischmann, Henning A. Höppe

Angaben zur Veröffentlichung / Publication details:

Schäfer, Martin J., Florian Fleischmann, and Henning A. Höppe. 2022. "On new alkaline earth hexafluorogermanates as host structures for UV phosphors." *Zeitschrift für anorganische und allgemeine Chemie* 648 (24): e202200309. https://doi.org/10.1002/zaac.202200309.

Journal of Inorganic and General Chemistry
ZAAC
Zeitschrift für anorganische und allgemeine Chemie
www.zaac.wiley-vch.de
RESEARCH ARTICLE

DOI: 10.1002/zaac.202200309

On New Alkaline-Earth Hexafluorogermanates as Host Structures for UV Phosphors

Martin J. Schäfer,[a] Florian Fleischmann,[a] and Henning A. Höppe*[a]

Herrn Prof. Dr. Rudolf Hoppe zum 100. Geburtstag gewidmet

Two new hexafluorogermanate dihydrates, viz. $SrGeF_6 \cdot 2H_2O$ and $CaGeF_6 \cdot 2H_2O$, were synthesised from aqueous solutions; their crystal structures were refined in space group $P2_1/n$ ($SrGeF_6 \cdot 2H_2O$: $a = 5.9605(2)$ Å, $b = 9.6428(3)$ Å, $a = 10.9866(3)$ Å and $\beta = 99.1590(10)$, $Z = 4$, 5122 refl., 104 param., $R_1 = 0.0195$, $wR_2 = 0.0470$; $CaGeF_6 \cdot 2H_2O$: $a = 5.8472(5)$ Å, $b = 10.5099(9)$ Å, $c = 9.6267(9)$ Å and $\beta = 103.521(3)$, $Z = 4$, 4756 refl., 101 param., $R_1 = 0.0224$, $wR_2 = 0.0616$). Upon doping with Eu^{2+} luminescence in the NUV regime was observed. The crystal structures of $CaGeF_6$ and $MgGeF_6$ could be solved and refined via Rietveld refinement from powder samples gained by thermal decomposition of the respective hydrates; both compounds adopt the $LiSbF_6$ structure type ($CaGeF_6$: $a = 5.4099(5)$ Å, $c = 13.9835(13)$ Å, $Z = 3$, $R_{wp} = 0.0291$, $R_{Bragg} = 0.0142$; $MgGeF_6$: $a = 5.1219(2)$ Å, $c = 13.0851(7)$, $Z = 3$, $R_{wp} = 0.034$, $R_{Bragg} = 0.01$). Further, the luminescence of $MgGeF_6 \cdot 6H_2O$:Eu^{2+}, which emits light in the violet to blue regime, is reported.

Introduction

Hexafluorogermanates, like their hexafluorosilicate analogues, have been a researched compound class for quite a long time.[1,2] While most representatives of these compound classes are simple to synthesise, some require elaborate synthesis techniques, as shown by the copper bombs of *Hoppe et. al.*,[3] or as published more recently, by high temperature reactions in fluorine atmosphere of *Kraus et al.*.[4] Hexafluorogermanates are often functionalised as red phosphors by doping with Mn^{4+}, since its allowed ^2E-$^4A^2$-transition is promising for applications in LED lightning and displays alike.[5,6] Since most hexafluorogermanates so far feature singly charged cations, tetravalent manganese was the only possible activator with efficient luminescence, although $BaGeF_6$ was successfully doped with Ce^{3+} and Tb^{3+} previously.[7] *Jüstel et al.* even used a Guanidinium complex as a counter cation for hexafluorogermanates doped with Mn^{4+}.[8] This work expands this family of compounds further by introducing strontium and calcium, both suited to host another very efficient activator, namely Eu^{2+}. As analogue host compounds for the hexafluorosilicates, $SrSiF_6 \cdot 2H_2O$ and $SrSiF_6 \cdot 2H_2O$ were reported by *Golovastikov et al.*[9] and *Frisoni et al.*, respectively.[10] $SrGeF_6 \cdot 2H_2O$ and $CaGeF_6 \cdot 2H_2O$ were, to our knowledge, never published before and so this publication aims to elucidate the syntheses, structures and thermal behavior of $SrGeF_6 \cdot 2H_2O$ and $CaGeF_6 \cdot 2H_2O$, their dehydrated forms $SrGeF_6$ and $CaGe_6$ and similar compounds like $MgGeF_6 \cdot 6H_2O$[11] and its dehydrated phase $MgGeF_6$, as well as the optical behaviour of Eu^{2+} and Mn^{4+} when doped into some these compounds.

While the already mentioned elaborate synthesis via solid state reaction in fluorine atmosphere is very well suited for doping with Mn^{4+}, these oxidizing conditions make doping with Eu^{2+} impossible, as it is very sensitive to oxidation during the formation of phosphors. Aqueous solutions can however be altered to achieve this doping, as shown in our contribution.

Results and Discussion

$SrGeF_6 \cdot 2H_2O$ crystallises in the monoclinic crystal system with space group $P2_1/n$, the lattice parameters are $a = 5.9605(2)$ Å, $b = 9.6428(3)$ Å, $a = 10.9866(3)$ Å and $\beta = 99.1590(10)$ (Figure 1a). There are four formula units per unit cell and all atoms occupy the Wyckoff position 4*e*. Non-condensed GeF_6 octahedra build up planes parallel to the *a*–*b*-plane. These octahedra are highly regular (Figure 1b), showing only 0.34% deviation from octahedral symmetry, as calculated according to the method suggested by *Balić-Žunić and Mackoviky*.[12,13] The Ge–F distances are in the range of 1.77 to 1.79 Å, slightly shorter than the sum of the two ionic radii (1.86 Å).[14] The F–Ge–F bond angles are very close to 90° (88.4–91.4°) for neighbouring and 180° (177.9–178.4°) for opposing atoms, as expected for such regular octahedra. The distance between germanium atoms is 5.14(2) Å, which might be relevant for an energy transfer or concentration quenching in possible future applications with Mn^{4+}.

[a] *M. J. Schäfer, F. Fleischmann, H. A. Höppe*
Lehrstuhl für Festkörperchemie
Institut für Physik, Universität Augsburg
Universitätsstraße 1, 86159 Augsburg
E-mail: henning@ak-hoeppe.de

Supporting information for this article is available on the WWW under https://doi.org/10.1002/zaac.202200309

Journal of Inorganic and General Chemistry
ZAAC
Zeitschrift für anorganische und allgemeine Chemie

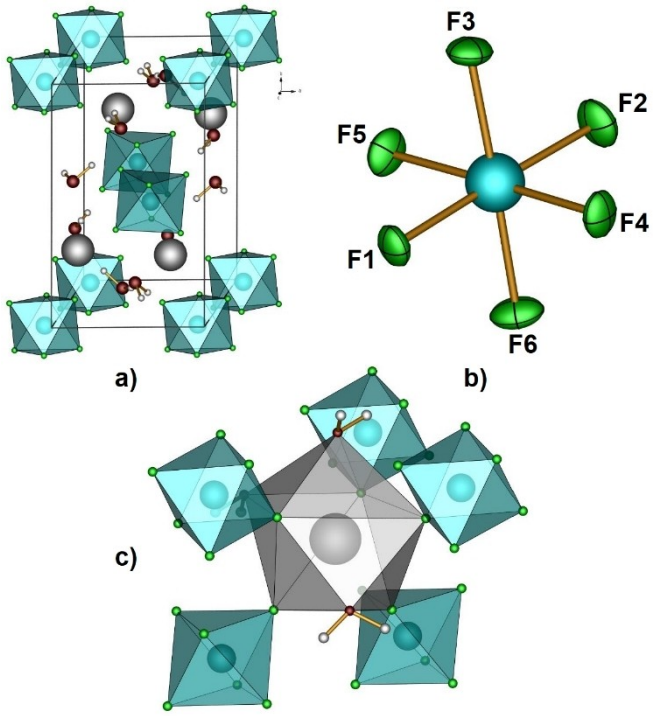

Figure 1. a) Unit cell of $SrGeF_6 \cdot 2H_2O$; b) regular GeF_6 octahedron with the one terminal F2 atom and the five fluorine atoms coordinating Sr; c) coordination environment of Sr^{2+} with five GeF_6 octahedra and three water molecules forming a distorted trigondodecahedron; strontium in light grey, germanium and GeF_6 octahedra in turquoise and fluorine in light green, displacement ellipsoids drawn at a 50% probability level.

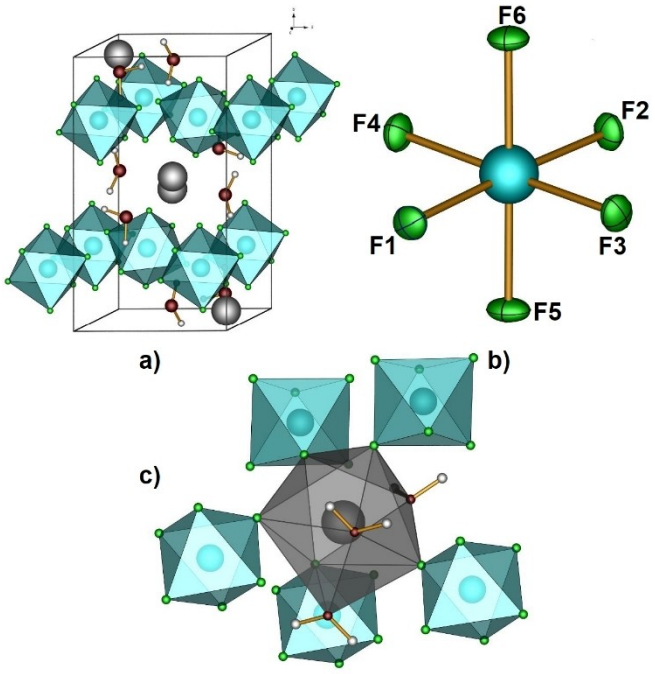

Figure 2. a) Unit cell of $CaGeF_6 \cdot 2H_2O$; b) regular GeF_6 octahedron with the one terminal F3 atom and the five fluorine atoms coordinating Ca; c) coordination environment of Ca^{2+} with five GeF_6 octahedra and three water molecules forming a distorted trigondodecahedron; calcium in grey, germanium and GeF_6 octahedra in turquoise and fluorine in light green, displacement ellipsoids drawn at a 50% probability level.

The Sr cations (Sr–Sr distance 4.37 Å) are situated in between these layers, as are the water molecules. Strontium is eightfold coordinated by five fluorine anions (Figure 1c), each by an individual GeF_6 octahedron and three water molecules. These water molecules are crystallographically different, as the molecule including OW1 bridges between two strontium cations, whereas the water molecule including OW2 only coordinates one strontium cation at a time. The designations "OW1" and "OW2" are given to the two oxygen atoms to indicate that they are oxygen atoms of crystal water, not of the anionic substructure. The interatomic distances Sr–F range between 2.44–2.52 Å and those of Sr–O between 2.60–2.69 Å. Both ranges vary around the sum of the respective ionic radii.[14] Among all six fluorine atoms, only F2 does not coordinate the strontium cation and can therefore be seen as truly terminal.

$CaGeF_6 \cdot 2H_2O$ crystallises monoclinically in the space group $P2_1/n$, like the strontium compound. Its lattice parameters are $a = 5.8472(5)$ Å, $b = 5.8472(5)$ Å, $c = 5.8472(5)$ Å and $\beta = 103.521(3)^\circ$ (Figure 2a). There are four formula units per unit cell and all atoms are situated on the general position 4*e*.

The structure is built up by layers of non-condensed GeF_6 octahedra, which are stacked parallel to the *a*-*c*-plane. The calcium cations and the water molecules are situated in between these layers. As in $SrGeF_6 \cdot 2H_2O$, the GeF_6 octahedra show a high regularity (1.33% deviation from the ideal octahedron) (Figure 2b), in which the Ge–F distances of 1.78–1.81 Å are once again slightly smaller than the sum of the ionic radii[14] but also minutely larger than the Ge–F distances in $SrGeF_6 \cdot 2H_2O$. The Ge–F distance is likely influenced by the charge density of the cation, with a smaller cation with a higher charge density pulling the fluorine atoms towards it. Since magnesium in $MgGeF_6 \cdot 6H_2O$ is surrounded by a shell of water molecules, it cannot be used in this comparison, but the Ge–F distance of 1.78 Å in $BaGeF_6$[15] supports this trend. The distances between neighbouring germanium atoms amounts to 5.03 Å.

The calcium cation is eightfold coordinated by five fluorine atoms (Figure 2c), each the corner of a separate GeF_6-octahedron and by three water molecules. As with the water molecules in $SrGeF_6 \cdot 2H_2O$, one water molecule (including OW2) bridges two coordination environments between calcium cations, the other (including OW1) only ever coordinated one Ca cation at a time. Ca–F distances range between 2.31–2.41 Å, Ca–O between 2.45–2.54 Å. Neighbouring Ca cations are 4.10 Å apart.

While the structures of both, $SrGeF_6 \cdot 2H_2O$ and $CaGeF_6 \cdot 2H_2O$, are very similar with respect to their identical space group or the same coordination motifs of all atoms, they are not isostructural. When the structure is set up according to convention ($\beta \neq 90^\circ$), the lattice parameters *b* and *c* are switched between both structures. The main differences are the

orientation of the octahedra in the structures and the location of the water molecules. Even if the structures are considered in the same setting of *a*, *b* and *c*, the direction along which their GeF_6 octahedra tilt is different. The transition between the two structures can be thought of as two different directions in which the octahedra are tilt from the undistorted case observed for $NaCrF_6$, which crystallises in the space group *Pnma*, a super group of $P2_1/n$[16] (Figure 3).

In $CaGeF_6 \cdot 2H_2O$ (left image in Figure 3), the water molecules line up along [010], while the water molecules in $SrGeF_6 \cdot 2H_2O$ (right image in Figure 3) appear to be drawn towards the heavy strontium atoms. These themselves are distorting the structure, compared to $CaGeF_6 \cdot 2H_2O$ to build up layers of cations and water molecules between the layers of GeF_6 octahedra. Further details on both structures, as well as their structure determination and refinement can be found in the supplement (Tables S1–S3 and S6-S8, respectively).

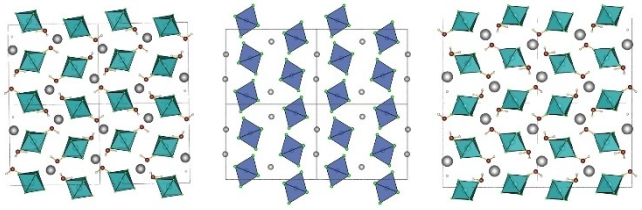

Figure 3. Extended unit cells of $CaGeF_6 \cdot 2\ H_2O$ (left) and $SrGeF_6 \cdot 2\ H_2O$ (right), the extended unit cell of $NaGeF_6$ in between to illustrate the tilting of the octahedra in two different directions; calcium in grey, sodium/strontium in light grey, chromium and CrF_6 octahedra in blue, germanium and GeF_6 octahedra in turquoise and fluorine in light green.

Figure 4 shows the IR spectra of in the range of 4000–400 cm^{-1}. In the case of all three compounds, the absorption bands around 3400–3600 cm^{-1} and around 1650 cm^{-1} can be attributed to stretching and deformation modes of water molecules[14] in the hydrated compounds $MGeF_6 \cdot 2H_2O$ (M = Ca, Sr) and $MgGeF_6 \cdot 6H_2O$. The dried compounds show no such bands or negligibly so, proving the successfully removed crystal water. In the case of $SrGeF_6 \cdot 2H_2O$, these bands did not occur even if the samples were stored under ambient laboratory conditions for weeks, aside from very small broad bands consistent with moisture adsorbed by the powder samples.

The common bands of all spectra are around 560 cm^{-1} and are attributed to the asymmetric stretching mode of Ge–F in the GeF_6 octahedra.[17] The stretching modes of Ge–O in GeO_2, a common side phase would be detected around 605 cm^{-1}. This allowed the detection of phase purity even if the potential amount of GeO_2 was too low to be detected by PXRD.

As shown in Figure 5, the thermal decomposition of the hexafluorogermanates discussed in this work has been observed and investigated. The decomposition always starts with the dehydration of the compounds, followed by the decomposition to the respective fluoride MF_2 (M = Mg, Ca, Sr) by releasing gaseous GeF_4. As shown, the bigger the cation, the softer it becomes as its charge density lowers and it may be polarised more easily, allowing for interactions with the anions and this increases the decomposition temperature. In the case of $MgGeF_6 \cdot 6H_2O$, an additional step which presumably corresponds to a dihydrate form $MgGeF_6 \cdot 2H_2O$, was observed in TG and VT-XRD measurements (see Figure S3 in the supplement), but the phase could so far not be isolated for an elucidation of its crystal structure.

The thermal decomposition of $CaGeF_6 \cdot 2H_2O$ and $MgGeF_6 \cdot 6H_2O$ yielded $CaGeF_6$ and $MgGeF_6$, respectively, the structures of which were not reported so far and shall be discussed in this work. Samples of dry $CaGeF_6$ and $MgGeF_6$ were

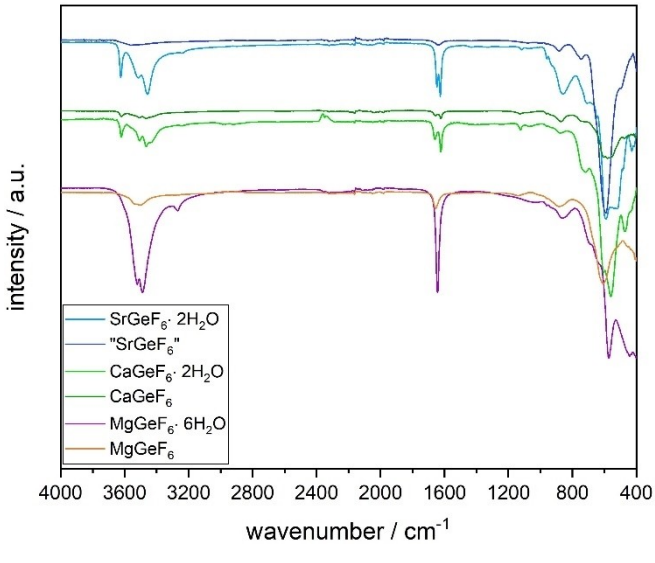

Figure 4. ATR-FT-IR spectra in the range of 4000–400 cm^{-1} of $MgGeF_6 \cdot 6H_2O$ (violet), $MgGeF_6$ (orange), $CaGeF_6 \cdot 2H_2O$ (light green), $CaGeF_6$ (dark green), $SrGeF_6 \cdot 2H_2O$ (light blue) and dehydrated $SrGeF_6$ (dark blue).

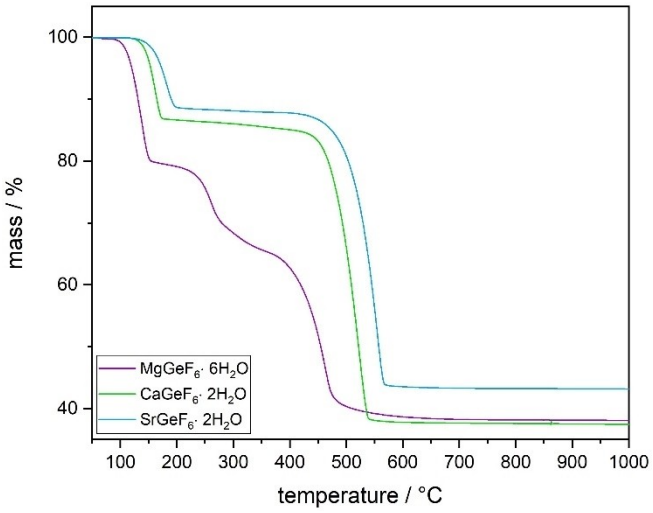

Figure 5. TGA curves between room temperature and 500 °C of $MgGeF_6 \cdot 6H_2O$ (violet), $CaGeF_6 \cdot 2H_2O$ (light green) and $SrGeF_6 \cdot 2H_2O$ (light blue).

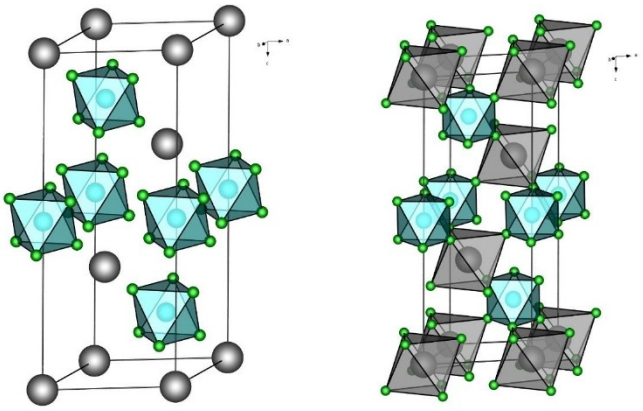

Figure 6. Unit cells of $CaGeF_6$ in the $LiSbF_6$ type (left) and once more with connected GeF_6 and CaF_6 octahedra; calcium and CaF_6 octahedra in gray, germanium and GeF_6 octahedra in turquoise and fluorine in light green.

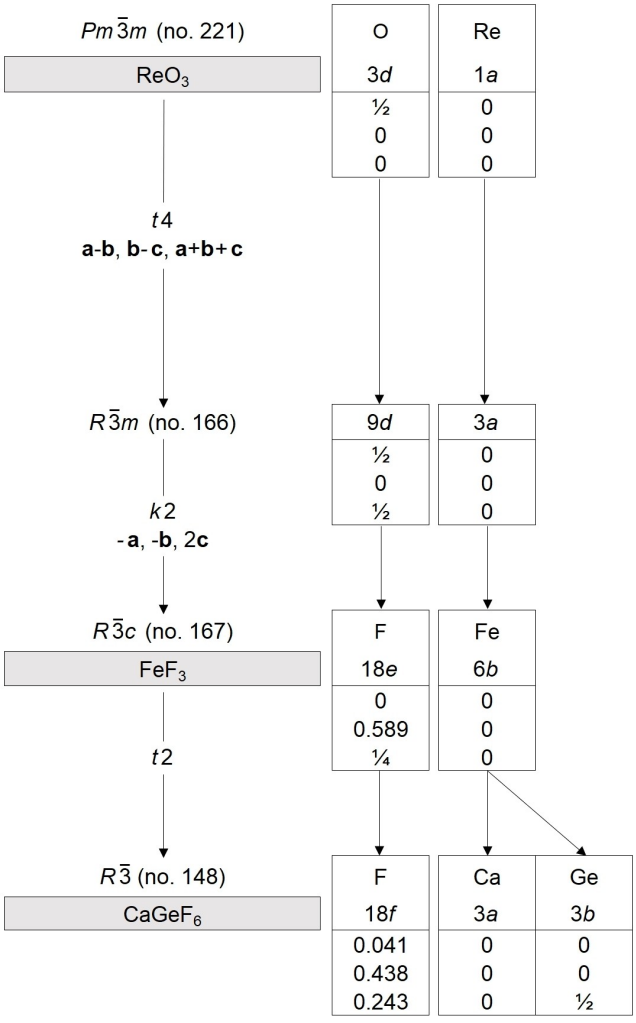

Figure 7. Symmetry relations according to the group-subgroup formalism after Bärnighausen[20,21] leading from the space group *Pm* $\bar{3}$*m* (e.g. ReO_3) to *R*$\bar{3}$, the space group of the $LiSbF_6$ type, in which $CaGeF_6$ and $MgGeF_6$ crystallise.

gained as residues from TG/DTA measurements, in situ during VT-XRD measurements or simply by drying the respective hydrated compounds in a compartment dryer overnight. The structure refinement was achieved by *Rietveld* refinement of capillary XRD (Figs. S1 and S4) on these dried samples. So far, no attempt to achieve the same for $SrGeF_6$ was successful, but an initial space group determination limits the selection of possible space groups to *R*$\bar{3}$, *R*32, *R*3 *m* or *R*$\bar{3}$*m*.

Both, $CaGeF_6$ and $MgGeF_6$, crystallise in a trigonal unit cell with space group *R*$\bar{3}$ in the $LiSbF_6$ structure type (Figure 6, left),[18] which itself is derived from the structure type of ReO_3 via a *t*4 transition to *R*$\bar{3}$3*m* and a subsequent *k*2 transition to give FeF_3,[19] which in turn yields *R*$\bar{3}$ by a further *t*2 transition (Figure S5). In the *Bärnighausen* scheme (Figure 7), this structural relationship is shown in more detail. The lattice parameters are $a = 5.4099(5)$ Å, $c = 13.9835(13)$ Å ($CaGeF_6$) and $a = 5.1219(2)$ Å, $c = 13.0851(7)$ Å ($MgGeF_6$), respectively. There are three formula units per unit cell, the alkaline earth cations occupy the Wyckoff positions 3*a*, the germanium atoms 3*b* and the fluorine anions are situated on the general positions 18*f*. GeF_6 and MF_6 (M = Mg, Ca) octahedra build up a three-dimensional network by corner-sharing in all three directions (Figure 6, right).

In $CaGeF_6$, the Ge–F distances of 1.79 Å are somewhat shorter than the sum of their ionic radii of 1.86 Å, and well in line with the Ge–F distances of $CaGeF_6 \cdot 2H_2O$. The Ca–F distance in the CaF_6 octahedra of 2.2124(3) Å is also slightly shorter than the sum of their ionic radii (2.285 Å).

In $MgGeF_6$, the Ge–F distances of 1.81 Å deviate only slightly from the sum of the ionic radii of 1.86 Å.[14] Compared to other hexafluorogermanates in this work, the charge density of Mg^{2+} without coordinating water is by far the highest and therefore, the GeF_6 octahedra are the largest. The Mg–F distance of 1.95 Å is only slightly shorter than the sum of the ionic radii of 2.005 Å.

According to the determined deviations of only 0.03% (GeF_6) and 0.0% (MgF_6) and 0.12% as well as 0.01% (CaF_6) in $CaGeF_6$ all octahedra can be classified as regular. Since the $LiSbF_6$ structure type is derived from the ReO_3 type (Figure 7), the deviations of the M^{2+}–F distances increase the larger their ionic radii get, as the ionic radius of Ge^{4+} of 0.53 Å stays the same in all the discussed structures and the structures seem to accommodate the respective ratio of ionic radii. As further argument might be considered that the increasing ionic radii of the alkaline earth cations put an increasing geometric pressure on the crystal structure, which is balanced by the shrinking of the GeF_6 octahedra; presumably even more probable, the increasing size of the cations reduces the electrostatic interaction between fluorine and alkaline earth cations. Details on both structures, as well as their structure determination and refinement can be found in the supplement (Tabs. S4-S5 and S9-S10 respectively).

To elucidate the hexafluorogermanates as host materials for Eu^{2+}, the two title compounds $SrGeF_6 \cdot 2H_2O$ and $CaGeF_6 \cdot 2H_2O$ were synthesized with one percent doping of Eu^{2+}. Mg was synthesized and doped as well for further comparison. All three fluorescence spectra of $Mg_{0,99}Eu_{0,01}GeF_6 \cdot 6H_2O$,

$Ca_{0,99}Eu_{0,01}GeF_6 \cdot 2H_2O$ and $Sr_{0,99}Eu_{0,01}GeF_6 \cdot 2H_2O$ (Figure 8) show some emission of trivalent europium, which was presumably oxidised during the synthesis, as Eu^{2+} is vulnerable to oxidation in aqueous solutions. The excitation and emission spectra of these traces of Eu^{3+} can be found in the supplement (Figure S8). In $Ca_{0,99}Eu_{0,01}GeF_6 \cdot 2H_2O$, the excitation wavelength is able to excite both, Eu^{2+} and Eu^{3+}, simultaneously, therefore, the bands between 550 and 750 nm attributed to trivalent europium's 4*f*–4*f* transitions are observed together with those of the 5*d*–4*f* transitions of the divalent species. To probe for traces of trivalent europium, the samples were excited with a wavelength of 393 nm, which selectively excites the Eu^{3+} species.

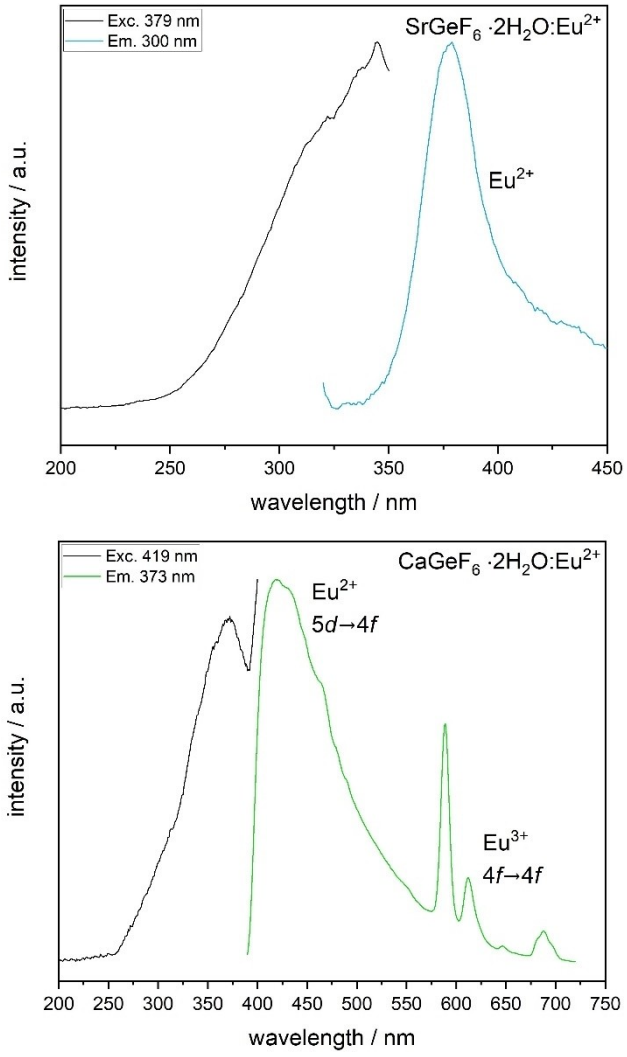

Figure 8. Fluorescence spectra of $Ca_{0,99}Eu_{0,01}GeF_6 \cdot 2H_2O$ and $Sr_{0,99}Eu_{0,01}GeF_6 \cdot 2H_2O$; $Sr_{0,99}Eu_{0,01}GeF_6 \cdot 2H_2O$ shows an excitation (black line, upper diagram) that was not possible to observe completely with the available experimental setup because of its position in the range around 200 nm; upon excitation, $Sr_{0,99}Eu_{0,01}GeF_6 \cdot 2H_2O$ shows emission (light blue line, upper diagram) in the UV region with a maximum around 379 nm; the excitation spectrum of $Ca_{0,99}Eu_{0,01}GeF_6 \cdot 2H_2O$ (black line, lower diagram shows the *f*-*d*-excitation in the UV with a maximum around 373 nm, leading to an emission (light green line, lower diagram) with a maximum around 419 nm, just outside the visible range.

However, the luminescence of divalent europium is the predominant emission in all three cases and shows a general redshift of the emission maxima, which is in concordance with the decreasing interatomic distance between the fluorine ligands and the metal cations strontium and calcium. This decreasing distance makes doping of magnesium compounds with divalent europium difficult, since the radius of Eu^{2+} (125 pm in eightfold coordination, 117 pm in sixfold coordination) fits perfectly on a position of Sr^{2+} (126 pm in eightfold coordination like in the title compound) and can still replace Ca^{2+} (112 pm in this case). The size discrepancy between Mg^{2+} and Eu^{2+} in the sixfold coordination (72 pm compared to 117 pm) seems to be too much for successful doping here. In addition, the magnesium cation is solely coordinated by six water molecules and the emission of $Mg_{0,99}Eu_{0,01}GeF_6 \cdot 6H_2O$ can therefore not be compared to the shared coordination by fluorine and water. Comparable to the emission of Eu^{2+} in other oxide (O^{2-} and H_2O) environments,[22,23] the hexahydrate surrounding of the europium cation forms an oscillator well-known to quench emission efficiently.[24] The resulting emission is very weak and any interpretation of the emission spectrum would be speculative. The recorded spectrum of $Mg_{0,99}Eu_{0,01}GeF_6 \cdot 6H_2O$ can be found in the supplement (Figure S7).

Concerning the maxima of the emission spectra of $Ca_{0,99}Eu_{0,01}GeF_6 \cdot 2H_2O$ and $Sr_{0,99}Eu_{0,01}GeF_6 \cdot 2H_2O$, the hexafluorogermanates can be ranked between borates and fluorooxoborates.[25,26] In the strontium compound, the emission maximum of 379 nm lies well within the UV region like that of the fluorooxoborate $SrB_5O_7F_3:Eu^{2+}$ (372 nm),[26] while the emission maximum of the calcium compound of 419 nm can be compared to weakly coordinating phosphates like $Sr_3(PO_4)_2:Eu^{2+}$ (420 nm),[27] concerning the coordination strength as host compounds. Depending on this coordination strength, Eu^{2+} is known to be able to emit light from the deep UV region like in $BaB_4O_6F_2$ (359 nm)[28] up to the deep red like in nitridosilicates like $M_2Si_5N_8$ (M = Eu, Sr, Ba) (581–641 nm)[29] or sulfides like CaS (645 nm).[30] Although the emissions peak in the violet to ultraviolet range of the electromagnetic spectrum, 4*f*–4*f* transitions could not be observed, which are reported for especially weak coordinating host structures like certain fluorooxoborates or halides.[31]

Conclusions

In our contribution we presented the crystal structures of the alkaline earth hexafluorogermanate hydrates $MGeF_6 \cdot 2H_2O$ (M = Ca, Sr) and of the anhydrous hexafluorogermanates, $MgGeF_6$ and $CaGeF_6$, obtained by careful thermal dehydration of the dihydrate and the hexahydrate $MgGeF_6 \cdot 6H_2O$. Unlike the latter or the anhydrous $BaGeF_6$, calcium and strontium form dihydrate compounds like their hexafluorosilicate analogues.[32–34] The thermal decomposition of the hydrates showed distinct steps

and so the structures of two new anhydrous hexafluorogermanates, $MgGeF_6$ and $CaGeF_6$ could be solved.

Doping with Eu^{2+} could be achieved in aqueous solution with a surprisingly simple setup and although some Eu^{3+} could be detected via fluorescence spectroscopy, viable spectra of Eu^{2+} were recorded and discussed. A rather early thermal decomposition prevents reduction of remaining Eu^{3+} ions.

Future experiments address the doping of our hexafluorogermanates $MgGeF_6 \cdot 6H_2O$, $MGeF_6 \cdot 2H_2O$ (M = Ca, Sr), $MGeF_6$ (M = Mg, Ca) and $BaGeF_6$ with Mn^{4+}, to achieve a co-doped phosphor with an efficient energy transfer between the spin- and parity allowed *d-f*-emission of Eu^{2+} and the *d-d*-transitions of Mn^{4+}.

Experimental Section

$SrGeF_6 \cdot 2H_2O$ was synthesized by reaction $SrCO_3$ (200.0 mg, 1.355 mmol) in a solution of H_2GeF_6, which was prepared in advance by stirring GeO_2 (141.6 mg,1.355 mmol) in a Teflon beaker and adding HF (50% solution, 0.353 ml, 8.130 mmol) dropwise to the suspension, resulting in a clear solution after an hour.

$CaGeF_6 \cdot 2H_2O$ was synthesized by reaction $CaCO_3$ (200.0 mg, 1.998 mmol) in a solution of H_2GeF_6, which was prepared in advance by stirring GeO_2 (209.0 mg, 1.998 mmol) in a Teflon beaker and adding HF (50% solution, 0.521 ml, 11.99 mmol) dropwise to the suspension, resulting in a clear solution after an hour. CaF_2 can occur as a side phase due to its high stability, but it can easily be removed by filtering the solution prior to drying it.

$MgGeF_6 \cdot 6H_2O$ was synthesized by reaction $MgCO_3$ (200.0 mg, 2.372 mmol) in a solution of H_2GeF_6, which was prepared in advance by stirring GeO_2 (248.1 mg, 2.372 mmol) in a Teflon beaker and adding HF (50% solution, 0.619 ml, 14.23 mmol) dropwise to the suspension, resulting in a clear solution after an hour.

In all three syntheses, phase purity was checked by powder X-ray diffraction. Even with intermediate filtering before the crystallization of the product, small traces of GeO_2 were often present in the final samples and could be detected both by powder PXRD and IR.

$M_{0.99}Eu_{0.01}GeF_6 \cdot 2H_2O$ (M = Ca, Sr) and $M_{g0.99}Eu_{0.01}GeF_6 \cdot 6H_2O$ were synthesized by the same method as the undoped samples, yet the water for the aqueous solution was degassed beforehand to prevent the oxidation of Eu^{2+} in the solution. This was achieved by supersonic treatment and bubbling srgon through the water in a round flask for one hour. $EuCO_3$ was used to substitute one percent of the alkaline earth carbonate during the synthesis.

***M*GeF$_6$ (M = Mg, Ca, Sr)** were prepared by decomposition of their respective dihydrates in a compartment dryer at 180 °C overnight. White, non-hygroscopic powder samples were gained and used without any further purification.

X-ray diffraction on single crystals were performed on suitable crystals which were selected under a polarizing microscope using a D8 venture diffractometer (MoK_α radiation, $\lambda = 0.7093$ Å or CuK_α radiation, $\lambda = 1.5406$ Å, depending on the crystals). Absorption correction was performed by the multi-scan method with the SAINT program within the Bruker APEX III program suite.[35] The structure was solved using Direct Methods and refined by using the OLEX2 software package,[36] as well as the SHELXTL crystallographic software[37] package for further refinement. Hydrogen atoms were located by identifying reasonable positions for protons in the difference Fourier syntheses. These could be further refined employing reasonable distance restraints. Crystallographic data and details of the measurement and refinement can be found in the supporting information. Further details of the crystal structure investigations may be obtained from the Fachinformationszentrum Karlsruhe, 76344 Eggenstein-Leopoldshafen, Germany (Fax: +49-7247-808-666; E-Mail: crysdata@fiz-karlsruhe. de, http://www.fiz-karlsruhe.de/request for deposited data.html) on quoting the depository numbers CSD-2207527 ($MgGeF_6$), CSD-2207528 ($SrGeF_6 \cdot 2H_2O$), CSD-2207529 ($CaGeF_6 \cdot 2H_2O$) and CSD-2207530 ($CaGeF_6$).

X-ray diffraction on powder samples was performed with a PANalytical Empyrean (Bragg-Brentano geometry using CuK_α radiation, a PIXcel 3D 2×2 detector, scan range: 5–70° 2θ, increment: 0.0263°, scan time 2127 s) and a Seifert 3003-TT (Bragg-Brentano geometry using CuK_α radiation, a GE METEOR 1D line detector, and a Ni-Filter to suppress K_β radiation, X-ray tube operated at 40 kV and 40 mA, scan range: 5–80° 2θ, increment: 0.02°, 40 scans per data point, integration time: 200 s per degree) at room temperature. All refinements were controlled for possible higher symmetries with Platon; while checkCIF suggested a possible pseudo symmetry for $CaGeF_6$ and the possible higher space group of $R\bar{3}c$, this was ruled out by Platon.[38] For the sake of completeness, a comparison of the observed XRD pattern of $CaGeF_6$ with the simulated patterns in our chosen space group as well as the space group proposed by checkCIF, can be found.

X-ray diffraction under inert atmosphere was performed by grinding the sample in a mortar inside of an Argon glovebox and filling it into a Hilgenberg glass capillary (either 0.3 or 0.5 mm diameter). VT-XTD was measured on the same diffractometer, but using quartz capillaries for higher temperature stability.

Infrared spectroscopy was measured with the ATR-FT method on a Bruker Equinox spectrometer in a range between 4000 and 400 cm^{-1}, the resolution was 4 cm^{-1}. Measurements were averaged over 32 individual scans.

Thermogravimetric analysis and differential thermal analysis were performed using a Netzsch Luxx, with corundum crucibles under nitrogen atmosphere in corundum crucibles Heating ramps varied within 5 and 10 K/min.

Acknowledgements

The authors acknowledge the distinguished contributions of Rudolf Hoppe to the broad field of solid-state chemistry, especially on the rich chemistry of fluorides and their manifold syntheses. Open Access funding enabled and organized by Projekt DEAL.

Conflict of Interest

The authors declare no conflict of interest.

Data Availability Statement

The data that support the findings of this study are available from the corresponding author upon reasonable request.

Keywords: divalent europium · UV phosphors · luminescence · germanates · fluorides

[1] J. L. Hoard, W. B. Vincent, *J. Am. Chem. Soc.* **1939**, *61(10)*, 2849.
[2] T. S. Khodashova, *Kristallografiya* **1957**, *2*, 609.
[3] F. Averdunk, R. Hoppe, *Z. Anorg. Allg. Chem.* **1990**, *582*, 111.
[4] J. Bandemehr, D. Baumann, M. Seibald, K. Eklung, A. Karttunen, F. Kraus, *Eur. J. Inorg. Chem.* **2021**, 3861.
[5] Y. K. Xu, S. Adachi, *J. Electrochem. Soc.* **2011**, *158(3)*, J58.
[6] S. Adachi, *ECS J. Solid State Sci. Technol.* **2020**, *9*, 016001.
[7] G. George, M. D. Simpson, B. R. Gautam, D. Fang, J. Peng, J. Wen, J. E. Davis, D. Ila, Z. Luo, *RSC Adv.* **2018**, *8*, 39296.
[8] F. Baur, D. Böhnisch, T. Jüstel, *ECS J. Solid State Sci. Technol.* **2020**, *9*, 046003.
[9] N. I. Golovastikov, N. V. Belov, *Kristallografiya* **1982**, *27(6)*, 1084.
[10] S. Frisoni, S. Brenna, N. Masciocchi, *Powder Diffr.* **2011**, *26(4)*, 308.
[11] J. Stepien-Damm, K. Lukaszewicz, R. Hrabánski, *Z. Kristallogr.* **1996**, *211*, 936.
[12] T. Balić Žunić, E. Makovicky, *Acta Crystallogr.* **1996**, *B52*, 78.
[13] E. Makovicky, T. Balić-Žunić, *Acta Crystallogr.* **1998**, *B54*, 766.
[14] R. D. Shannon, *Acta Crystallogr.* **1976**, *A32*, 751.
[15] J. L. Hoard, W. B. Vincent, *J. Am. Chem. Soc.* **1940**, *62(11)*, 3126.
[16] Z. Mazej, E. Goreshnik, *Eur. J. Inorg. Chem.* **2008**, 1795.
[17] J. Weidlein, U. Müller, K. Dehnicke, *Schwingungsfrequenzen I – Hauptgruppenelemente*, Georg Thieme Verlag, Stuttgart, New York, **1981**.
[18] J. H. Burns, *Acta Crystallogr.* **1962**, *15*, 1098.
[19] M. Leblanc, J. Pannetier, G. Ferey, R. de Pape, *Rev. Chim. Miner.* **1985**, *22*, 107.
[20] H. Bärnighausen, *MATCH* **1980**, *9*, 139.
[21] U. Müller, *Z. Anorg. Allg. Chem.* **2004**, *630*, 1519.
[22] S. Shionoya, W. M. Yen, H. Yamamoto, *Phosphor Handbook*, 2nd Edition, CRC Press, Boca Raton, **2017**, p. 146.
[23] J. Sommerdijk, A. Bril, *J. Lumin.* **1976**, *11*, 363.
[24] L. Song, Y.-W. Wu, W.-X. Chai, Y.-S. Tao, C. Jiang, Q.-H. Wang, *Eur. J. Inorg. Chem.* **2015**, 2264.
[25] P. Dorenbos, *J. Phys. Condens. Matter* **2003**, *15*, 575.
[26] M. J. Schäfer, S. G. Jantz, H. A. Höppe, *Z. Naturforsch.* **2020**, *75(1)*, 143.
[27] S. H. M. Poort, J. W. H. van Krevel, R. Stomphorst, A. P. Ving, G. Blasse, *J. Sol. State Chem.* **1996**, *122*, 432.
[28] S. G. Jantz, F. Pielnhofer, L. van Wüllen, R. Weihrich, M. J. Schäfer, H. A. Höppe, *Chem. Eur. J.* **2018**, *24*, 443.
[29] a) H. A. Höppe, H. Lutz, P. Morys, W. Schnick, A. Seilmeier, *J. Phys. Chem. Solids* **2000**, *61*, 2001–2006; b) R. Mueller-Mach, G. Mueller, M. R. Krames, H. A. Höppe, F. Stadler, W. Schnick, T. Juestel, P. Schmidt, *Phys. Status Solidi A* **2005**, *202*, 1727–1732; c) M. Zeuner, F. Hintze, W. Schnick, *Chem. Mater.* **2009**, *21(2)*, 336.
[30] C. Guo, D. Huang, Q. Su, *Mat. Sci. Eng.* **2006**, *B130*, 189.
[31] J. L. Sommerdijk, P. J. Verstegen, A. Bril, *J. Lumin.* **1974**, *8(6)*, 502.
[32] S. Syoyama, K. Osaki, *Acta Crystallogr.* **1972**, *B28*, 2626.
[33] S. Frisoni, S. Brenna, N. Masciocchi, *Powder Diffr.* **2011**, *26(4)*, 308.
[34] N. I. Golovastikov, N. V. Belov, *Kristallografiya* **1982**, *27(6)*, 1084.
[35] *APEX3*, Version 2016.9-0, Bruker AXS Inc., **2016**.
[36] *OLEX2*, Version 1.3-ac4, Rigaku Oxford Diffraction, **2019**.
[37] G. Sheldrick, *SHELXTL*, Version 6.14, Bruker AXS, **2003**.
[38] A. L. Spek, *Acta Crystallogr. Sect. D* **2009**, *65*, 148.

Manuscript received: September 15, 2022
Revised manuscript received: November 4, 2022
Accepted manuscript online: November 7, 2022

